Earth and Planetary Science Letters 388 (2014) 387–398

Contents lists available at ScienceDirect

Earth and Planetary Science Letters

www.elsevier.com/locate/epsl

A 4.2 billion year old impact basin on the Moon: U–Pb dating of zirconolite and apatite in lunar melt rock 67955

Marc D. Norman [a,b,*], Alexander A. Nemchin [c]

[a] Lunar and Planetary Institute, 3600 Bay Area Boulevard, Houston, TX 77058, USA
[b] Research School of Earth Sciences, Australian National University, Mills Road, Canberra, ACT 0200, Australia
[c] Department of Applied Geology, Curtin University of Technology, Perth, WA 6845, Australia

ARTICLE INFO

Article history:
Received 7 February 2013
Received in revised form 19 November 2013
Accepted 19 November 2013
Available online 11 January 2014
Editor: T.M. Harrison

Keywords:
Moon
terminal cataclysm
late heavy bombardment
geochronology
zirconolite
apatite

ABSTRACT

A sharp rise in the flux of asteroid-size bodies traversing the inner Solar System at 3.9 Ga has become a central tenet of recent models describing planetary dynamics and the potential habitability of early terrestrial environments. The prevalence of ~3.9 Ga crystallization ages for lunar impact-melt breccias and U–Pb isotopic compositions of lunar crustal rocks provide the primary evidence for a short-lived, cataclysmic episode of late heavy bombardment at that time. Here we report U–Pb isotopic compositions of zirconolite and apatite in coarse-grained lunar melt rock 67955, measured by ion microprobe, that date a basin-scale impact melting event on the Moon at 4.22 ± 0.01 Ga followed by entrainment within lower grade ejecta from a younger basin approximately 300 million yr later. Significant impacts prior to 3.9 Ga are also recorded by lunar zircons although the magnitudes of those events are difficult to establish. Other isotopic evidence such as ^{40}Ar–^{39}Ar ages of granulitic lunar breccias, regolith fragments, and clasts extracted from fragmental breccias, and Re–Os isotopic compositions of lunar metal is also suggestive of impact-related thermal events in the lunar crust during the period 4.1–4.3 Ga. We conclude that numerous large impactors hit the Moon prior to the canonical 3.9 Ga cataclysm, that some of those pre-cataclysm impacts were similar in size to the younger lunar basins, and that the oldest preserved lunar basins are likely to be significantly older than 3.9 Ga. This provides sample-based support for dynamical models capable of producing older basins on the Moon and discrete populations of impactors. An extended period of basin formation implies a less intense cataclysm at 3.9 Ga, and therefore a better opportunity for preservation of early habitable niches and Hadean crust on the Earth. A diminished cataclysm at 3.9 Ga suggests that the similarity in the age of the oldest terrestrial continental crust with the canonical lunar cataclysm is likely to be coincidental with no genetic significance.

© 2013 Elsevier B.V. All rights reserved.

1. Introduction

Large impacts on the early Earth and the other terrestrial planets must have exerted a powerful influence on surficial environments and thermal structures (Zahnle et al., 2007; Abramov and Mojzsis, 2009), but the timing, duration, and magnitude of this early bombardment, and its consequences for planetary evolution, are poorly constrained. The concept of a cataclysmic spike in the impact flux between 3.8 and 4.0 Ga was developed to explain the age distribution of lunar impact-melt breccias and a ubiquitous 3.9 Ga metamorphic overprint on U–Pb isotopic compositions of lunar crustal rocks (Tera et al., 1974; Ryder, 2002; Stöffler et al., 2006). Shock events of similar ages in meteorites from Mars (Beard et al., 2013) and a variety of asteroidal parent bodies (Bogard, 2011) imply that a pulse of heavy bombardment traversed the inner Solar System at that time. In contrast, evidence for a heavy bombardment of the Earth has been elusive (Ryder et al., 2000), which is surprising considering the expected intensity and duration of the terrestrial infall extrapolated from the lunar record. Recently, Abbott et al. (2012) reported evidence for a heating event in 3.85–3.95 Ga detrital zircons compared to older grains, whereas Bell and Harrison (2013) found a statistically anomalous population of low-T metamorphic zircons with ages of 3.84–3.91 Ga. Both studies suggested that these effects might be related to large impacts on the Earth, although endogenic mechanisms could not be excluded (cf. Wielicki et al., 2012).

Studies of the Moon and lunar samples have been critical for defining the concept of a late heavy bombardment. Crater populations require an intense phase of post-accretionary bombardment that declined rapidly after ~3.6 Ga (Strom et al., 2005), but the timing of this barrage and the absolute ages of lunar basins are not further constrained by those data. Subtle but resolvable differences in the ^{40}Ar–^{39}Ar ages of melt breccias linked with lunar basins (Dalrymple and Ryder, 1996), and the recognition of discrete melt-forming impact events during the interval 3.8–4.0 Ga

* Corresponding author.

0012-821X/$ – see front matter © 2013 Elsevier B.V. All rights reserved.
http://dx.doi.org/10.1016/j.epsl.2013.11.040

(Norman et al., 2006), support the concept of a late heavy bombardment, but whether this represents a short, sharp spike in the impact flux or a longer-lived epoch of basin formation is an open question with significant implications for solar system dynamics (Gomes et al., 2005), early planetary environments (Abramov and Mojzsis, 2009), and biological evolution (Chyba and Sagan, 1992; Farmer, 2000; Ryder, 2002; Marty and Meibom, 2007).

The absence of crystalline impact melt rocks with ages older than 4.0 Ga has been cited as a key piece of evidence favoring a late cataclysm (Ryder, 2002). In this scenario, several, and perhaps all, of the ~50 lunar basins (>300 km diameter) formed during a unique spike in the arrival of asteroid-size impactors some 500–700 million yr after planetary accretion. Rapid migration of resonances through the Kuiper and asteroid belts in response to orbital reconfiguration of the outer planets provides a plausible mechanism for a late cataclysm (Gomes et al., 2005), although other mechanisms such as destruction of older deposits during an extended period of high impact flux (Hartmann, 2003) are viable alternative explanations for the narrow range of lunar impact-melt breccia ages. Distinguishing between these alternatives would contribute toward a better understanding of solar system evolution (Morbidelli et al., 2000) and predictions of habitability in exoplanetary systems (Lisse et al., 2012).

Until recently, isotopic dating of lunar impacts relied almost exclusively on ^{40}Ar–^{39}Ar ages of clast-poor, crystalline melt rocks (Bogard, 1995; Norman et al., 2006; Jourdan, 2012; Fernandes et al., 2013). These analyses can, however, be complicated by the presence of relict clasts, incomplete outgassing, diffusive modification during shock and heating associated with younger impacts, and exposure to solar wind and cosmic rays on the lunar surface (Fernandes et al., 2013). U–Pb dating of accessory phases such as zircon and apatite offers another perspective on lunar impact history (Pidgeon et al., 2007; Grange et al., 2011; Joy et al., 2011; Zhang et al., 2012). Here we present new U–Pb isotopic data for zirconolite and apatite from a crystalline lunar melt rock (sample 67955) that provide definitive evidence for a basin-scale impact event on the Moon at least 300 million yr prior to the youngest lunar basins. This direct evidence for a post-accretionary basin-forming impact on the Moon implies a much longer duration for the late heavy bombardment than typically assumed.

2. Material and methods

2.1. Breccia 67955

The Apollo 16 mission collected 67955 to sample a large, white clast within a massive boulder of dark, melt-matrix breccia (Outhouse Rock) situated on the rim of North Ray crater. This boulder represents the deepest of two layers excavated by North Ray crater, underlying a more porous unit of lightly welded, fragmental matrix breccias that were also sampled at this station. The dark-matrix breccias appear to have experienced a higher degree of shock welding than the light-matrix fragmental breccias, but still much lower than that recorded by crystalline lunar melt rocks. Petrographic observations suggest that these dark and light matrix breccias are composed of similar materials shocked to different intensities (Stöffler et al., 1985), and the distinctly aluminous compositions and similar abundances of incompatible elements in both types of breccia support this idea. These breccias were likely emplaced as a heterogeneously welded unit of distal impact ejecta during a basin-forming event (Hodges et al., 1973).

Sample 67955 is composed of lithic clasts of a crystalline noritic anorthosite lithology in a matrix of comminuted mineral fragments. The lithic clasts have poikilitic textures with pyroxene oikocrysts enclosing euhedral to subhedral crystals of olivine and plagioclase. Mineral compositions in the lithic clasts and the fragmental matrix are uniform and identical, indicating that the matrix formed by in-situ crushing of the noritic anorthosite (Hollister, 1973; Ashwal, 1975). 67955 appears to have been a monolithologic crystalline rock that was variably shocked, fractured, and partially recrystallized (Nord et al., 1975), but relatively large lithic clasts with well-preserved crystalline textures remain and one of these was sampled for this study. A 1.87 g sample (67955,78) was allocated for geochemistry and geochronology, and a polished thin section (67955,85) was prepared from an adjacent piece of the same clast.

In thin section, the sample we studied is holocrystalline with an unbrecciated, poikilitic to glomerocrystic igneous texture consisting of predominantly equant, euhedral to subhedral plagioclase and olivine surrounded by anhedral oikocrysts of pyroxene (Fig. 1).

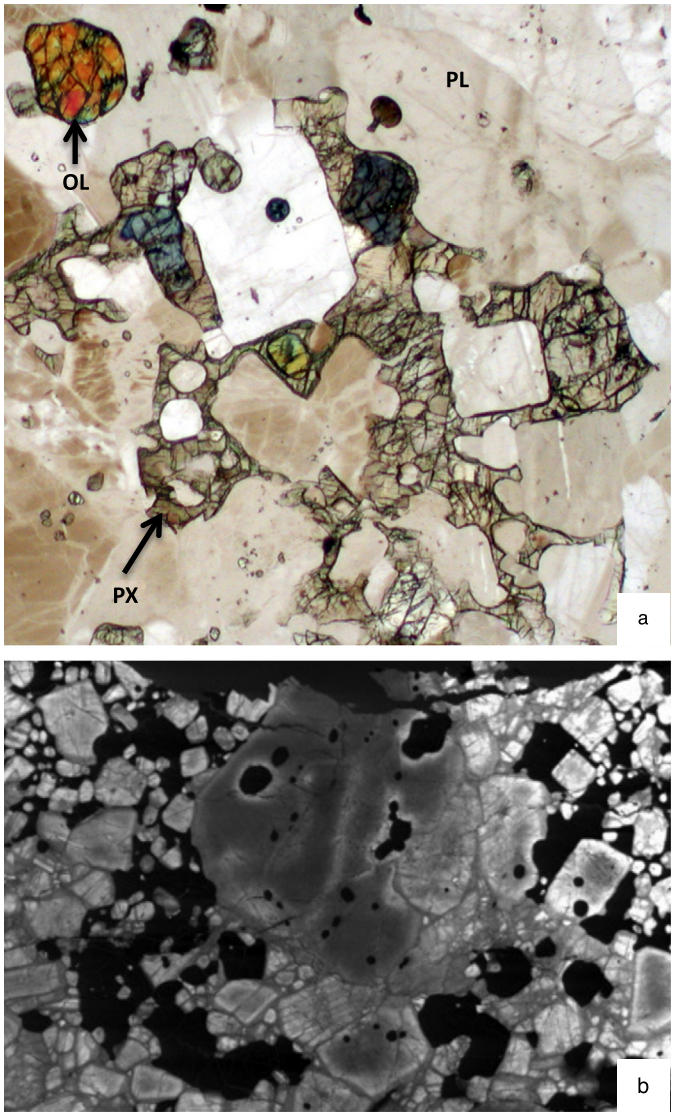


Fig. 1. Petrographic characteristics of 67955,85. The clast analyzed for this study has a coarse-grained, slightly annealed, poikilitic texture consistent with slow crystallization of a silicate melt. (a) Transmitted light optical photomicrograph of thin section 67955,85 illustrating euhedral to subhedral crystals of plagioclase (PL) and olivine (OL) enclosed by poikilitic pyroxene (PX). Field of view is 1×1 mm. (b) SEM-CL image of 67955,85. Euhedral plagioclase grains tend to be concentrically zoned consistent with growth from a melt. The larger, irregularly shaped plagioclase grains have patchy, CL-dark cores that lack concentric relationships with crystal faces. These grains are interpreted as relict, undigested clasts of plagioclase. The large dark grain in the center of the field of view is ~1 mm wide. Black interstitial areas are predominantly pyroxene and olivine.

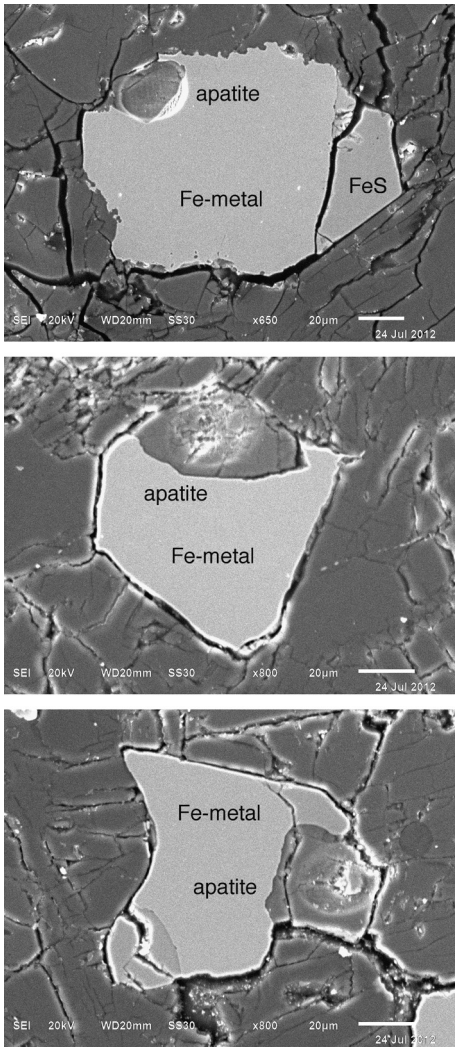


Fig. 2. SEM-BSE images of Fe-metal grains with associated apatite and FeS in thin section 67955,85. Note ion microprobe spots on the apatites.

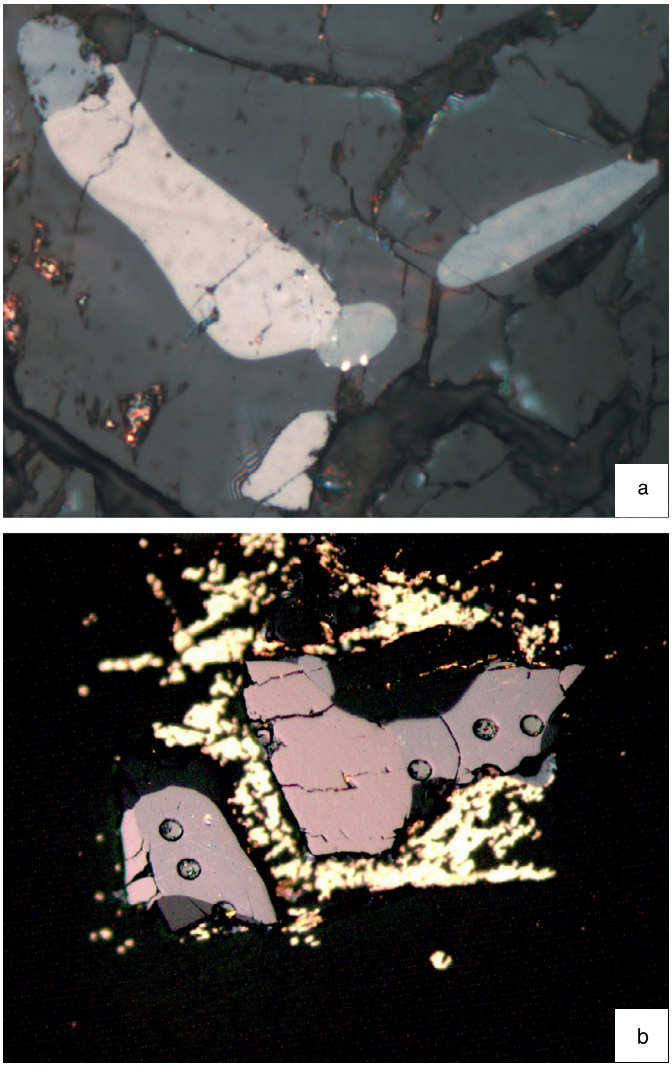


Fig. 3. Reflected light photomicrographs of ilmenite (pink) and associated zirconolite (gray) assemblages in 67955. (a) In thin section 67955,85. The large ilmenite grain is ~50 µm long. The assemblage occurs within a pyroxene near a grain boundary with plagioclase. The bright spots on the edge of the zirconolite in the center of the field of view are sulfide blebs. (b) Composite grains in a polished epoxy mount. Ion microprobe spots are visible on the zirconolite grains. The bright material surrounding the grains is residual Au coat from the ion microprobe analysis.

Section ,85 consists of 69.8 vol% plagioclase and 29.4 vol% mafic silicates, which is somewhat more mafic than the mode reported by Hollister (1973) with 78.5 vol% plagioclase, 20.5 vol% mafic silicates (14.5% pyroxene, 6.0% olivine) and 1 vol% metal. Pyroxene oikocrysts are up to 300–400 µm long and the widths of euhedral to subhedral plagioclase grains range from ~40 to 400 µm, averaging ~100–200 µm. Polysynthetic twinning and spherical inclusions of olivine are common in the plagioclase, and SEM-CL images typically show concentric zoning in the euhedral grains (Fig. 1, Supplementary Materials). In contrast, several of the larger plagioclase grains (up to ~1 mm) are irregularly shaped and have diffuse, asymmetric patterns of CL response in their cores (Fig. 1); this type of plagioclase comprises ~10–20 vol% of the section studied here. Relict clasts of pyroxene or olivine are absent, and there are no identifiable xenoliths within the noritic anorthosite lithology. Most of the plagioclase has a patchy extinction and fine-scale internal dislocations consistent with mild shock, but the primary crystalline texture of the sample has not been disrupted by fracturing or brecciation.

Ilmenite, Cr-spinel, Fe-metal, phosphate (apatite), sulfide (FeS), and a Zr–Ca–Ti oxide identified as zirconolite are present as accessory phases (0.3 vol% oxides; 0.5 vol% metal + sulfides). Apatite was reported previously by Hollister (1973) but zirconolite had not been recognized in this rock prior to our study. Apatite occurs as euhedral to subhedral grains often physically associated with Fe-metal (Fig. 2); the analyzed grains were typically ~20 µm. Zirconolites analyzed for this study ranged from ~30 to 250 µm in long dimension. In thin section, zirconolite occurs as anhedral grains either enclosed by pyroxene or interstitial to the pyroxene and plagioclase. Most of the zirconolites analyzed here were found in a polished mount of polymineralic grains separated during handpicking of mineral separates. Petrographic relationships in these composite grains suggest a common association of zirconolite with ilmenite (Fig. 3). Inclusions of zirconolite or apatite within plagioclase or olivine have not been observed. SEM-CL imaging of the zirconolites did not reveal any compositional zoning or other internal features, possibly due to quenching by Fe.

2.2. Methods

Major element compositions of zirconolite were measured by electron microprobe. Trace element compositions of apatite and zirconolite grains were measured by laser ablation ICPMS using the NIST 612 glass to calibrate relative mass intensities. Individual laser

ablation analyses were normalized to 57.5 wt% CaO for apatite and 9.4 wt% CaO for zirconolite measured on ^{43}Ca to correct for variable ablation yields. Concentrations of highly siderophile elements in Fe-metal grains were determined by LA-ICPMS using the Lombard hexahedrite and the NIST 610 glass for intensity calibration (Gilbert et al., 2012) with normalization to 6.9 wt% Ni measured on ^{61}Ni.

U–Pb isotopic data were collected using the SHRIMP II ion microprobe at Curtin University. The filtered O_2^- primary ion beam was reduced through a 70 µm Köhler aperture to obtain a spot diameter of ~10 µm and an intensity of ~1.1 nA. Each analysis was preceded by a 2-min raster to remove surface contamination. The peak-hopping routine for apatite consisted of ten scans through the mass stations, with signals measured by an electron multiplier. A large apatite crystal (BRA-1) with an age of 2058 Ma and 67 ppm U was used as the reference for ^{238}U/^{206}Pb, calibrated using linear relationships of ln(^{206}Pb/^{238}U) vs. ln(^{238}U^{16}O/^{238}U). It is difficult to establish the slopes of the lines for individual ion probe sessions as the variation of ^{238}U^{16}O/^{238}U is small, so a slope of 1.85 defined by BRA-1 analyses collected during the last five years was used to correct all lunar apatites. Four grains of apatite from the Duluth gabbro returned a concordia age of 1150 ± 59 Ma (MSWD = 2.9) compared to the FC1 zircon age of 1099 ± 1 Ma (Supplementary Material).

Spot size and primary beam were further reduced for zirconolite analyses (~0.3 nA primary beam, 30 µm Köhler aperture) to minimize potential damage to the multiplier due to high U–Th concentrations. Previous SHRIMP studies of zirconolite (Rasmussen and Fletcher, 2004; Rasmussen et al., 2008, 2009) found that the Zr_2O^+ reference peak was too weak for accurate peak centering. Consequently, a procedure involving high to low mass stepping through the mass stations was adopted by those authors. We found that the Zr_2O^+ mass on the 67955 zirconolites was sufficiently intense to allow accurate peak centering, so a standard protocol of low to high mass peak hopping was adopted. In the absence of an independently calibrated zirconolite reference, U/Pb isotope ratios measured by SHRIMP cannot be used for age calculations so all zirconolite ages reported here are based on ^{207}Pb/^{206}Pb, which is insensitive to the specific mineral analyzed. The OG1 zircon (Stern et al., 2009) was used to monitor the reproducibility of ^{207}Pb/^{206}Pb and estimate U and Th concentrations. While a systematic error on these concentrations might be present, their relative magnitudes are robust. All errors of individual analyses of both apatite and zirconolite are presented as 1SD, whereas the mean ages are calculated as 95% confidence limit.

3. Results

3.1. Major and trace element compositions

The zirconolites contain 35–39% ZrO_2, 35–36% TiO_2, 7–10% CaO, 3–5% FeO, and percent level abundances of Y and Nb (Supplementary Material). The one zirconolite grain analyzed by laser ablation ICPMS for trace elements had high contents of normally incompatible lithophile elements, with REE abundances ranging from ~1100 × CI for La to ~13 000 to 15 000 × CI for the middle HREE (Gd–Er), a deep negative Eu anomaly (Fig. 4), and ~1.8 wt% yttrium (Supplementary Material). U–Th concentrations in this grain were ~1500 ppm and 4700 ppm, respectively. This grain also had high concentrations of Nb (7800 ppm), Ta (420 ppm), and Hf (3800 ppm) but low concentrations of Sr and Ba (~10 ppm each). Apatite contained ~700–2000 × CI of LREE with a negative Eu anomaly (Fig. 4; Supplementary Material). U–Th concentrations in these apatites were 2.5–6.1 ppm and 10–30 ppm, respectively, while Sr contents were relatively low (140–150 ppm). Highly siderophile element compositions of 67955 metal grains

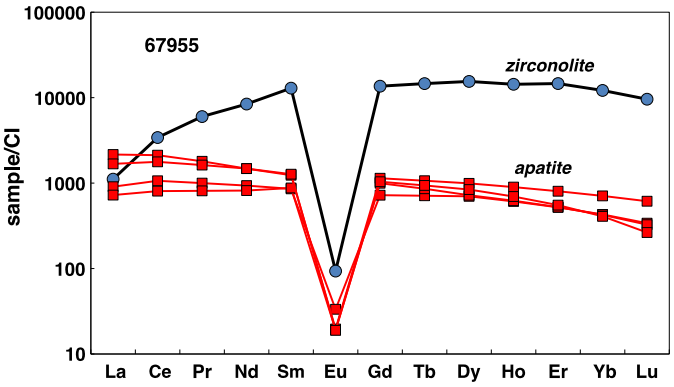


Fig. 4. REE patterns for apatite (squares) and zirconolite (circles) grains from 67955 normalized to the CI chondrite composition (Anders and Grevesse, 1989).

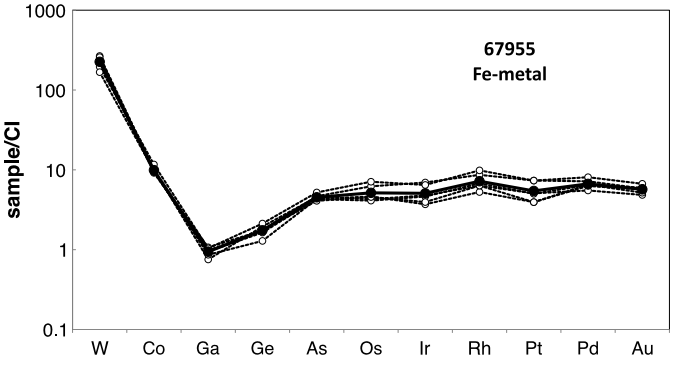


Fig. 5. Siderophile trace element composition of Fe-metal grains from 67955 normalized to the CI chondrite composition (Anders and Grevesse, 1989). Dashed lines with open symbols are the individual analyses presented in Table S4, and the solid line with filled symbols is the average of these analyses.

have approximately chondritic relative abundances for platinum-group elements, Au, and As, slight relative depletions in Ga and Ge, a slight enrichment in Co and a strong enrichment in W relative to the CI-normalized PGE abundances (Fig. 5; Supplementary Material).

3.2. U–Pb isotopic compositions and ages

Zirconolites measured by ion microprobe had high and variable U and Th contents, ranging from 516–14 800 ppm and 1110–40 700 ppm, respectively (Table 1; Fig. 6). ^{207}Pb/^{206}Pb ages of the zirconolites are correlated with their U + Th concentrations, such that grains with lower U + Th yielded older ages and grains with higher U + Th returned predominantly younger ages (Fig. 6). The main group of low-U (<2000 ppm) grains with ages of 4.20–4.25 Ga has a weighted mean age of 4.22 ± 0.01 Ga (Fig. 6; $n = 9$). In contrast, zirconolites with higher U (⩾6000 ppm) have predominantly younger ^{207}Pb/^{206}Pb ages between 3.93 and 4.09 Ga (Fig. 6). Three analyses (85-4-1, 85-4-2, E89-2) returned ^{207}Pb/^{206}Pb ages ⩾4.3 Ga and do not fall along the trend just described (Table 1; Fig. 6). Apatite has much lower uranium concentrations, mostly ⩽10 ppm. ^{207}Pb/^{206}Pb ages of apatites range between 4201 ± 37 and 4022 ± 68 Ma (Table 2; Fig. 7). Although a concordia intercept age of 4.13 ± 0.04 Ga can be calculated for these apatites (Fig. 7), the unrealistically small MSWD of 1.6 for this intercept compared to the range of ^{207}Pb/^{206}Pb ages obtained for individual apatites (4.02–4.20 Ga) reflects the relatively large errors in the individual age determinations.

Table 1
Pb isotopic compositions and U–Th concentrations of 67955 zirconolite. Spot numbers marked with an asterisk were used for the weighted mean age (Ma). $^{207}Pb^*/^{206}Pb^*$ ratios are 204-corrected for common Pb.

Grain #	Spot #	U (ppm)	Th (ppm)	$^{204}Pb/^{206}Pb$	err (%)	$^{207}Pb/^{206}Pb$	err (%)	$^{208}Pb/^{206}Pb$	err (%)	$^{207}Pb^*/^{206}Pb^*$	err (%)	$^{207}Pb/^{206}Pb$ age	err (Ma)
PTS, 85													
1	1	11 851	33 883	0.000001	49	0.4336	0.4	0.6368	0.3	0.4336	0.4	4030	±6
1	2	12 159	38 328	0.000002	41	0.4237	0.4	0.5874	0.1	0.4237	0.4	3996	±6
2	1	13 744	36 210	0.000004	41	0.4333	0.1	0.6094	0.2	0.4333	0.1	4029	±1
2	2	13 575	37 547	0.000002	41	0.4203	0.5	0.6127	0.5	0.4202	0.5	3983	±7
3	1	14 788	40 731	0.000006	30	0.4436	0.3	0.6006	0.4	0.4435	0.3	4064	±4
3	2	11 208	37 718	0.000001	45	0.4433	0.3	0.6005	0.2	0.4433	0.3	4063	±4
4	1	1371	2683	0.000019	35	0.5562	0.4	0.4209	0.5	0.5561	0.4	4397	±6
4	2	1121	2400	0.000013	38	0.5189	0.6	0.3999	0.5	0.5189	0.6	4296	±9
4	3*	1423	2845	0.000022	32	0.4877	0.2	0.3965	1.4	0.4875	0.2	**4204**	±4
4	4*	1773	3592	0.000009	45	0.4887	0.2	0.4151	0.3	0.4887	0.2	**4207**	±3
4	5*	1350	2601	0.000008	41	0.4938	0.2	0.3723	0.5	0.4938	0.2	**4223**	±3
4	6*	1607	3086	0.000000	45	0.4946	0.2	0.3750	0.4	0.4947	0.2	**4226**	±4
6	1*	1452	2763	0.000020	33	0.4914	0.2	0.3720	0.3	0.4913	0.2	**4215**	±3
6	2*	1300	2518	0.000028	35	0.5014	0.2	0.4243	0.4	0.5012	0.2	**4245**	±4
Grain mount													
C68	1	9097	20 840	0.000006	46	0.4166	0.6	0.5052	0.9	0.4166	0.6	3970	±9
C68	2	8201	16 000	0.000004	40	0.4050	0.5	0.3979	0.4	0.4049	0.5	3928	±7
C68	3	10 482	31 685	0.000000	0	0.4083	0.4	0.6371	0.3	0.4083	0.4	3940	±6
C68	4	12 162	35 731	0.000000	0	0.4168	0.6	0.6151	1.0	0.4168	0.6	3971	±9
C68b	1	6953	22 679	0.000003	41	0.4323	0.2	0.6971	0.8	0.4323	0.2	4025	±2
C68b	2	6339	21 654	0.000004	41	0.4451	2.5	0.7419	0.8	0.4451	2.5	4069	±37
C68b	3	13 799	27 585	0.000000	0	0.4221	0.7	0.4410	0.5	0.4221	0.7	3990	±10
C68b	4	10 703	21 778	0.000003	71	0.4110	0.1	0.4293	0.6	0.4110	0.1	3950	±2
C12	1*	516	1110	0.000032	38	0.4914	0.3	0.4215	0.4	0.4912	0.3	**4215**	±4
C12	2*	639	1177	0.000035	35	0.4976	0.3	0.3782	0.5	0.4974	0.3	**4233**	±4
C71	1	5832	22 904	0.000005	35	0.4386	1.2	0.7968	1.1	0.4385	1.2	4047	±17
C71	2	8657	13 910	0.000007	28	0.4064	0.1	0.3351	0.4	0.4064	0.1	3933	±2
C71	3	5838	23 192	0.000005	42	0.4752	0.8	0.7891	0.4	0.4752	0.8	4166	±12
C71	4	8049	28 544	0.000003	41	0.4374	0.5	0.7070	0.6	0.4373	0.5	4043	±7
C71	5	7557	28 855	0.000014	39	0.4501	0.6	0.7603	0.3	0.4500	0.6	4085	±9
C71a	1	6165	25 065	0.000005	38	0.4223	0.3	0.8888	0.3	0.4223	0.3	3990	±5
C71a	2	8994	32 101	0.000020	29	0.4228	0.6	0.7779	1.2	0.4227	0.6	3992	±10
C71a	3	6435	25 100	0.000008	30	0.4178	1.0	0.8831	0.8	0.4177	1.0	3974	±14
C71a	4	7990	31 072	0.000000	0	0.4262	0.9	0.8198	0.5	0.4262	0.9	4004	±13
C71a	5	7826	35 218	0.000004	54	0.4229	0.4	0.8627	0.3	0.4229	0.4	3992	±6
E89	1	9696	12 461	0.000002	40	0.4214	0.7	0.2795	0.6	0.4214	0.7	3987	±10
E89	2	11 117	16 266	0.000005	27	0.5249	2.9	0.3079	0.7	0.5249	2.9	4313	±43
E89	3	9142	28 355	0.000011	45	0.4254	1.5	0.6226	1.7	0.4253	1.5	4001	±23
E89	4	7380	22 189	0.000004	33	0.4247	0.4	0.6303	0.7	0.4247	0.4	3999	±6
E89	5	7546	23 410	0.000004	38	0.4307	2.5	0.6962	0.7	0.4306	2.5	4020	±37
F90	1	4161	20 202	0.000003	47	0.4832	0.3	1.0530	0.3	0.4831	0.3	4191	±5
F90	2	4410	19 757	0.000014	41	0.4917	0.4	0.9636	0.8	0.4916	0.4	4216	±6
F90	3	4065	19 061	0.000008	38	0.4884	0.2	1.0024	0.9	0.4884	0.2	4207	±3
F90	4	5378	29 131	0.000000	0	0.4958	0.5	1.1910	0.5	0.4958	0.5	4229	±7
F90	5	4740	24 323	0.000000	0	0.4886	0.3	1.1271	0.3	0.4886	0.3	4207	±4
F4	1*	832	2257	0.000015	41	0.4945	0.2	0.5018	0.4	0.4944	0.2	**4225**	±3

4. Discussion

4.1. Origin of 67955: an impact melt rock

Early petrologic studies of 67955 noted the crystalline igneous texture and homogeneous mineral compositions of the noritic anorthosite, and concluded that it formed by slow cooling of a silicate melt followed by annealing, shock brecciation, and injection of glass veins (Hollister, 1973; Ashwal, 1975; Nord et al., 1975). Hollister (1973) concluded that a silicate melt was required to account for the homogeneous mineral compositions, the high equilibration temperature (>900 °C) and the poikilitic texture, but was unable to distinguish an origin by impact melting vs. endogenic magmatism. Ashwal (1975) also favored an origin by crystallization of a silicate melt, and recognized both the high siderophile element concentrations and abundance of Fe-metal, but he concluded that these were primary characteristics of an endogenic magma. Warner et al. (1977) classified the rock as a 'feldspathic granulitic impactite', emphasizing its metamorphic aspects. Cushing et al. (1999) classified it as a 'poikilitic granulite' and suggested that this textural type of lunar granulite formed by impact melting.

67955 obviously had a complex history, but we conclude that the textural and compositional characteristics of the crystalline noritic anorthosite lithology that we studied are more consistent with an origin by impact melting rather than endogenic magmatism. The abundance of euhedral, concentrically zoned plagioclase and subhedral olivine (Fig. 1), the poikilitic texture, and the homogeneous mineral compositions (Hollister, 1973; Ashwal, 1975) are consistent with crystallization of a melt phase comprising ~80–90% of the rock. We interpret the irregularly-shaped plagioclase grains with dark, diffuse SEM-CL structures (Fig. 1) as undigested clasts, which implies ~10–20 vol% of relict plagioclase. Clast populations in lunar impact melt rocks become increasingly dominated by plagioclase as the abundance of clasts decreases due to preferential digestion of pyroxene, olivine, and

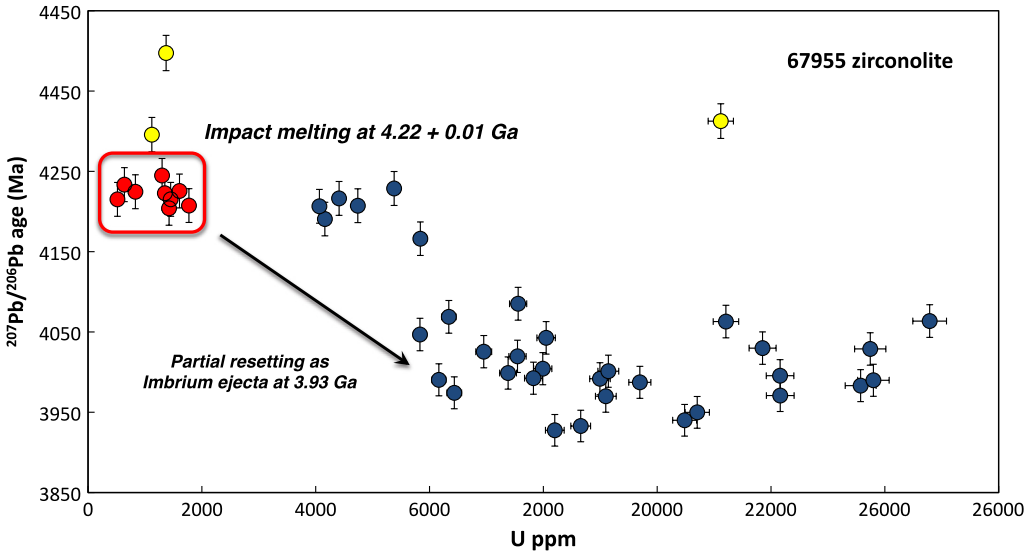


Fig. 6. SHRIMP U–Pb data for zirconolite grains from 67955. $^{207}Pb/^{206}Pb$ ages of the zirconolites are correlated with their U and Th contents. The cluster of low-U grains (red symbols) record the primary crystallization age of this melt rock at 4.22 ± 0.01 Ga. High-U grains (blue symbols) received a more intense time-integrated alpha dose and therefore were prone to losing radiogenic Pb during entrainment of 67955 within younger basin ejecta at ~3.9 Ga. Yellow symbols may reflect incorporation of unsupported lunar crustal Pb (see text for discussion). Errors are 2% on concentrations and 0.5% in isotope ratios.

oxides (Simonds, 1975; Simonds et al., 1976; Warner et al., 1976), and the poikilitic textured lunar melt rocks have the most refractory (i.e., plagioclase-rich) clast populations, consistent with high initial temperatures of equilibration (Simonds et al., 1973, 1976; Supplemental Material). In the interpretation presented here, the 67955 noritic anorthosite impact melt would have a clast-melt equilibration temperature near that of the liquidus of its bulk composition.

In addition to its petrographic characteristics, the abundance and composition of Fe-metal in the noritic anorthosite demonstrates the presence of significant meteoritic contamination. The Ni–Co composition of this metal lies within the 'meteoritic' field (Ashwal, 1975) and is distinct from that of endogenic plutonic rocks of the lunar crust, which contain scarce amounts of Fe-metal with predominantly non-meteoritic Ni/Co (Ryder et al., 1980). The unbrecciated nature of our sample and the textural characteristics of the metal grains (Figs. 1, 2) show that the metal was present during crystallization of the melt rather than, for example, being introduced by physical mixing of meteoritic metal into a metal-poor cumulate. The composition and abundance of this Fe-metal implies ~250–300 ppm Ni and ~6–9 ppb Ir (~1–3% CI) in the bulk rock, similar to previously measured splits of 67955 (see Meyer, 2010). These concentrations are typical of lunar impact melt rocks (Palme, 1980) and much higher than those of endogenic plutonic rocks of the lunar crust, which have intrinsically low concentrations of siderophile elements ($<3 \times 10^{-4}$ CI; Warren, 1993; Day et al., 2010). The approximately chondritic relative abundances of siderophile elements in the metal grains (Fig. 5) are consistent with the presence of a significant meteoritic component. The strong enrichment of W and the more modest enrichment of Co relative to the PGE indicate incorporation of lunar W and Co into the metal during the impact-melting event that formed the 67955 noritic anorthosite (Wänke et al., 1978; Delano and Ringwood, 1978; Anders, 1978).

Finally, the bulk composition of 67955 as reflected both in its modal mineralogy and in its major element abundances also distinguishes it from the known suites of endogenic lunar highlands cumulates. For example, the subequal abundance of pyroxene and olivine in 67955 contrasts with the mineralogical characteristics of the endogenic cumulates, which are either (gabbro)norites with little olivine, or troctolites with little pyroxene (Norman and Ryder, 1979; James, 1980). These differences are reflected in its modal plagioclase abundance (70–80 vol%) and, equivalently, its Al_2O_3 content (26–28 wt%; Meyer, 2010), which are unlike those of the endogenic cumulates and instead are similar to those of polymict lunar breccias that formed by impact mixing (Ryder, 1979; James, 1980; Supplementary Materials). MELTS modeling of a 67955 bulk composition with 27 wt% Al_2O_3 at $fO_2 = IW$ returns a liquidus temperature of ~1325 °C, multiple saturation with plagioclase and olivine at ~1255 °C, and a solidus near 1125 °C. Assuming 20 vol% unmelted relict plagioclase lowers the liquidus by ~25 °C. Experimentally determined phase relationships on lunar compositions similar to 67955 (27–29 wt% Al_2O) obtained somewhat higher temperatures of crystallization (liquidus ~1380–1420 °C, solidus ~1200–1250 °C; Walker et al. 1972, 1973; see also Delano, 1977). The absence of clasts of pyroxene and olivine in 67955 together with the predominance of euhedral, concentrically zoned plagioclase (Fig. 1), the homogeneous mineral compositions, and the high pyroxene equilibration temperatures (Hollister, 1973; Ashwal, 1975) lead us to the conclusion that 67955 was a high-degree (80–90%) melt, and this melt crystallized at temperatures of ⩾1250–1300 °C.

Based on the combination of (1) the presence of relict clasts of plagioclase, (2) meteoritic contamination, and (3) its bulk composition, we conclude that the compositional and petrographic characteristics of the 67955 noritic anorthosite are distinct from those of endogenic cumulates of the lunar highlands, and are best understood by interpreting 67955 as a clast-poor, holocrystalline impact melt rock that was monomictly brecciated, slightly annealed and cut by late-stage fractures and glass after its primary crystallization.

A comparison with other lunar impact melt rocks in the Apollo sample collection suggests that the 67955 noritic anorthosite formed from a large effective volume of melt. Its intergranular texture lacks mesostasis or interstitial glass, and the plagioclase morphology is more equant than commonly observed in lunar impact melt rocks (Supplementary Materials; see also Norman et al., 2006). Qualitatively, these textural characteristics are consistent with slower cooling of the 67955 melt over the crystallization interval. Although the exact relationships between bulk composition, cooling rate, degree of under-cooling, and nucleation density are not precisely calibrated, relative cooling rates esti-

Table 2
U–Th–Pb isotopic compositions of 67955 apatite. Age in Ma. Each grain was analyzed with one spot only. $^{207}Pb^*/^{235}U$ and $^{206}Pb^*/^{238}U$ ratios have been corrected for common Pb.

Grain name	$^{204}Pb/^{206}Pb$	err (%)	$^{207}Pb/^{206}Pb$	err (%)	$^{208}Pb/^{206}Pb$	err (%)	U (ppm)	Th (ppm)	Th/U	$^{238}U/^{206}Pb$	err (%)	$^{207}Pb^*/^{235}U$	err (%)	$^{206}Pb^*/^{238}U$	err (%)	ρ	$^{207}Pb/^{206}Pb$ age	err (Ma)
Monte	0.00185	25	0.478	2.3	1.122	2.0	5	25	5.2	1.10	4.6	56.4	5.3	0.88	4.7	0.875	4134	±38
Pacman	0.00312	28	0.485	2.4	1.305	2.5	3	16	6.1	1.07	5.8	56.4	6.8	0.88	6.0	0.889	4129	±46
Frank	0.00291	45	0.491	2.7	1.038	3.1	2	9	4.4	0.86	7.2	71.1	8.5	1.09	7.6	0.894	4153	±56
Mike	0.00073	59	0.443	2.5	1.323	2.5	3	20	6.3	0.99	6.1	60.3	6.7	1.00	6.1	0.912	4044	±41
Key West	0.00190	53	0.457	3.1	1.117	3.3	2	10	5.3	0.88	7.3	66.6	8.5	1.09	7.6	0.890	4061	±58
Bunny	0.00022	24	0.464	1.1	4.601	5.8	30	624	21.5	1.07	2.7	59.3	2.9	0.93	2.7	0.926	4124	±16
Hap	0.00263	22	0.504	2.1	1.091	2.1	4	19	5.2	1.00	6.6	63.6	7.2	0.95	6.7	0.937	4201	±37
Chef	0.00003	99	0.484	1.5	1.073	1.7	6	32	5.1	1.09	3.9	60.9	4.2	0.91	3.9	0.936	4192	±22
Pat	0.00000	38	0.462	1.3	0.425	4.1	12	22	1.9	0.87	3.7	73.2	3.9	1.15	3.7	0.940	4126	±20
Crater	0.00049	31	0.458	0.9	0.385	1.3	74	116	1.6	0.96	2.8	64.5	2.9	1.03	2.8	0.949	4100	±14
TS85-1	0.00845	35	0.524	4.6	1.312	4.8	1	8	7.6	0.74	12.4	73.4	16.5	1.14	14.1	0.851	4136	±129
TS85-2	0.00646	21	0.510	2.3	1.946	7.0	2	18	9.2	0.73	8.5	76.8	9.8	1.20	9.0	0.917	4134	±58
TS85-3	0.00791	17	0.491	2.5	0.743	3.1	3	8	2.8	0.72	7.4	70.4	9.2	1.18	8.0	0.871	4022	±68

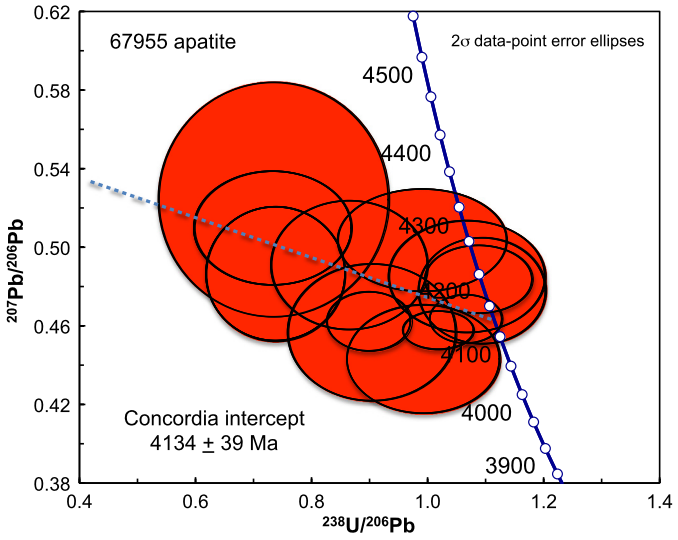


Fig. 7. A Tera-Wasserburg Concordia plot of U–Pb isotopic compositions in apatite from lunar sample 67955. Ellipses correspond to 2-sigma errors and reflect ratios uncorrected for initial Pb. The dashed line represents a projection of the best fit through the data in 3D ($^{238}U/^{206}Pb$–$^{207}Pb/^{206}Pb$–$^{204}Pb/^{206}Pb$ coordinates) onto the Concordia plane.

mated from olivine morphology (Donaldson, 1976; Faure et al., 2003) and plagioclase morphology and grain size (Cashman, 1993; Lesher et al., 1999) would be ~10 × slower for 67955 than for typical subophitic and fine-grained poikilitic Apollo 16 impact melt rocks over the temperature interval at which these phases crystallized from the melt. For average plagioclase growth rates of 10^{-8} to 10^{-9} cm/s, which are appropriate for slowly cooled lunar basalts (Cashman, 1993), an average plagioclase grain width of 100 μm (Section 2.1) would correspond to a crystallization interval of ~10–100 days.

In this framework, the 67955 noritic anorthosite represents one of the slowest cooled lunar melt rocks, and therefore one of the largest volumes of impact melt recognized so far in the lunar sample collection. As the crystalline Apollo melt breccias are generally considered to have formed by large impacts rather than small craters, with at least some if not most having been formed by basin-scale events (Warren et al., 1996; Norman et al., 2010; Warren, 2011), we conclude that the impact that formed the 67955 melt rock was similarly large, if not larger, and likely of a scale analogous to that of a lunar basin. Although smaller craters (e.g., 20 km diameter) are more numerous on the lunar surface, the formation of 67955 and other lunar melt rocks in smaller craters is less likely due to the proportionally larger volumes and greater thicknesses of melt produced by lunar basins (Warren et al., 1996; Cintala and Grieve, 1998; Abramov et al., 2012). In detail, there appears to be no perfect textural analogue for 67955 among terrestrial impact melt deposits, probably due to differences in bulk composition and volatile contents, but the petrographic characteristics of 67955 appear most analogous to those of crystalline melt rocks associated with the largest terrestrial impact structures such as the central melt sheet of Manicouagan (O'Connell-Cooper and Spray, 2011), the Sudbury norites (Naldrett et al., 1970; Therriault et al., 2002), and some hypidiomorphic varieties of granophyre dikes at the Vredefort structure (Reimold and Gibson, 2006) rather than deposits associated with smaller craters (cf. French, 1998). Our interpretation is that the crystalline noritic anorthosite lithology in 67955 formed in a large, slowly cooled volume of clast-poor impact melt in a setting analogous to a central melt sheet or proximal over-rim ejecta deposit produced by a large, likely basin-scale impact on the Moon.

4.2. Crystallization and entrainment ages of 67955

The occurrence of U-rich accessory phases such as zirconolite and apatite provides an opportunity to constrain the age and subsequent thermal history of the 67955 noritic anorthosite. Although zirconolite is a common accessory mineral in lunar mare basalts (Lovering and Wark, 1971; Haines et al., 1971; Peckett et al., 1972), it has not been widely used for geochronology due in part to its small grainsize. Early ion microprobe studies showed that it was possible to obtain meaningful age information from Pb isotopic compositions of these phases (Anderson and Hinthorne, 1972; Anderson and Hinthorne, 1973; Hinthorne et al., 1979). More recently, Rasmussen et al. (2008) and Zhang et al. (2010) dated zirconolite and other Zr-bearing phases in mare basalt 10047 and lunar meteorites MIL05035 and LAP02224, respectively. Terrestrial zirconolite is most commonly associated with alkaline or carbonatite complexes, kimberlites, and some hydrothermal systems, and it has been used to obtain precise ages of terrestrial mafic dikes and sills (Rasmussen and Fletcher, 2004; Rasmussen et al., 2009). It appears to be unstable during high-grade metamorphism, reacting to form zircon, titanite, and rutile in terrestrial crustal rocks (Pan, 1997), and it rarely, if ever, occurs as magmatic xenocrysts (Rasmussen et al. 2008, 2009; Wu et al., 2010). Lunar apatite and other phosphates such as whitlockite and merrilite have also been used for dating lunar basalts and impact breccias (Anand et al., 2003; Terada et al., 2007; Nemchin et al., 2009; Joy et al., 2011), although the relatively low closure T of the U–Pb system in these minerals makes them prone to isotopic resetting during subsequent thermal events (Anand et al., 2003; Nemchin et al., 2009).

We interpret both the apatite and the zirconolite in this sample of 67955 as primary accessory phases that crystallized in situ from late-stage residual melts rather than relict clasts. Although some endogenic lunar norites and troctolites do contain accessory phases such as ilmenite, zircon, apatite, whitlockite, and baddeleyite that might be incorporated as clasts into an impact melt (Dymek et al., 1975; James and Flohr, 1983; Zhang et al., 2012), zirconolite is quite rare and occurs only as small grains (<10 μm) in mesostasis assemblages that would have been readily assimilated by the impact melt. Based on its relative abundance in lunar breccias and endogenic igneous highlands rocks, zircon might be expected to be the most common relict accessory phase, and relict zircon has been identified in some clast-rich lunar impact breccias (Grange et al., 2011). However, no zircon was found in our sample of 67955.

Ilmenite, apatite, and zirconolite require wt% levels of elements such as Ti, P, and Zr to crystallize from a basaltic magma (Hess et al., 1978; Watson, 1979; Loiseau et al. 2003a, 2003b) and so would have been strongly undersaturated in a melt approximating the composition of 67955 with ~0.3 wt% TiO_2, <0.1 wt% P_2O_5, and ~60 ppm Zr (see Meyer, 2010). Ilmenite dissolves rapidly in undersaturated basaltic melts (Wagner and Grove, 1997; Van Orman and Grove, 2000) such that a 100 μm crystal would dissolve within a few hours at temperatures of 1250–1300 °C compared to the crystallization interval of ~10–100 days for the 67955 melt estimated from plagioclase grain size. We are not aware of analogous dissolution rate data for zirconolite but experimental studies show that it reacts rapidly to baddeleyite in silicate melts at the crystallization temperatures estimated for 67955 (Loiseau et al., 2003b) and so would be unlikely to survive as relict clasts in a slowly cooled impact melt. Apatite is somewhat more refractory but would still dissolve within at most ~4 days (see Harrison and Watson, 1984), which is a factor of >2–25 less than the crystallization interval for 67955 estimated from average plagioclase crystal size (Section 4.1). Preservation of relict zirconolite and apatite grains inherited from pre-impact crustal rocks also seems unlikely based on the absence of pyroxene and olivine clasts in 67955, as those silicate phases would be more refractory than either zirconolite or apatite and digested by the melt at a higher temperatures than the accessory phases, as seen in Apollo 17 impact melt breccias (Simonds, 1975; Warner et al., 1976). The lack of inclusions of either apatite or zirconolite in early-formed minerals such as plagioclase and olivine also mitigates against a relict origin for these U-bearing phases.

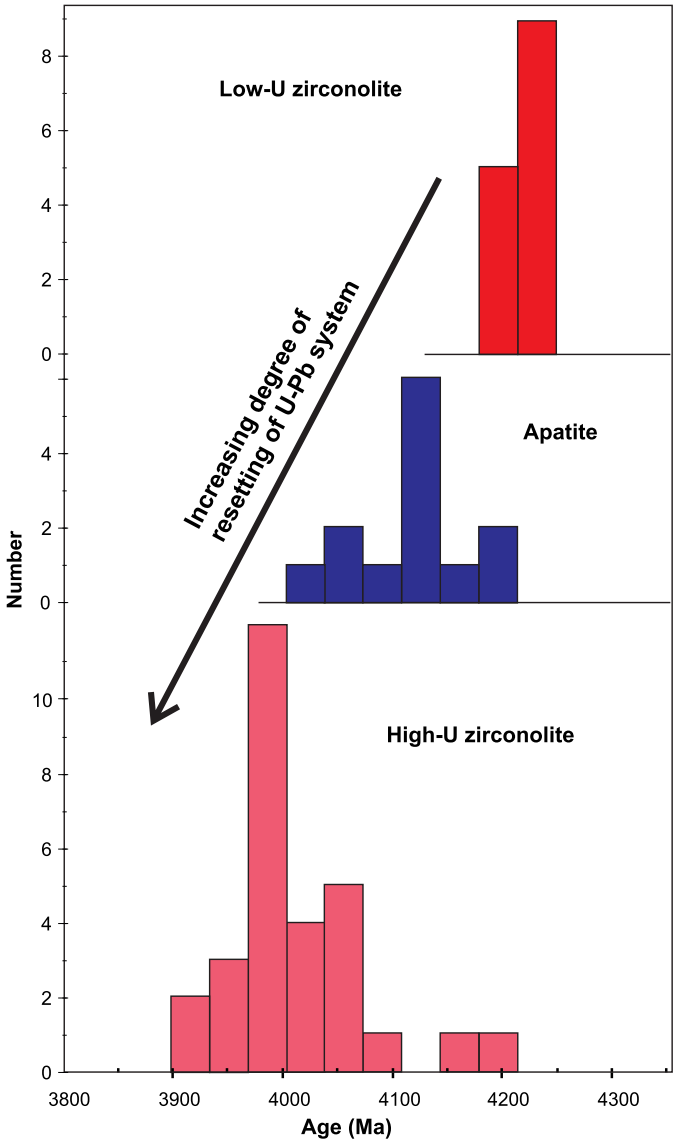


Fig. 8. A comparison of $^{207}Pb/^{206}Pb$ ages for zirconolite and apatite from 67955. Zirconolites with lower uranium contents record ages that cluster around 4.2 Ga whereas zirconolites with higher uranium contents tend to have younger ages that extend to as young as 3.9 Ga, Apatite ages are intermediate between those of the high-U and low-U zirconolites. We interpret these characteristics as reflecting variable resetting of the U–Pb isotopes, with the low-U zirconolites preserving the primary impact-melting age of 67955 and the apatites and high-U zirconolites being variably reset during entrainment in younger basin ejecta at ~3.9 Ga.

The coincidence of ages obtained from the low-U zirconolites (4.22 ± 0.01 Ga), the oldest apatite (4.20 ± 0.04 Ga), and the ^{147}Sm–^{143}Nd plagioclase-pyroxene mineral isochron reported by Norman et al. (2007; 4.20 ± 0.07 Ma) makes a strong case for a crystallization age of 4.2 Ga, which would make 67955 the oldest lunar impact melt rock dated so far. The low-U zirconolites provide the most precise estimate of the crystallization age of 67955 at 4.22 ± 0.01 Ga. Based on our interpretation of 67955 as a slowly-cooled impact melt, this would date the formation of a lunar basin at that time. The instability of zirconolite during

thermal metamorphism supports our conclusion that the sample of 67955 studied here was not strongly metamorphosed since it formed. We interpret the systematically younger $^{207}Pb/^{206}Pb$ ages in the high-U zirconolites and the intermediate ages of the apatites as recording variable Pb loss from these phases during a younger, relatively mild thermal event plausibly related to incorporation of 67955 into the fragmental ejecta unit from which it was sampled at the Apollo 16 site. In this interpretation, the high-U zirconolites were more completely reset than most of the apatites (Fig. 8). Although Pb diffusion in zirconolite has not been quantified experimentally, Pb loss is expected to be easier from metamict zirconolite than from crystals that have experienced less time-integrated radiation damage. Alpha dose calculated for the low-U zirconolite during the interval 4.2 to 3.9 Ga ranges between 0.15×10^{16} and 0.80×10^{16} a/mg. This is close to the critical dose when this mineral becomes amorphous at ambient temperature (Lumpkin et al., 1986). In contrast, the high-U zirconolites would have accumulated an order of magnitude greater alpha dose (2×10^{16} to 7×10^{16} a/mg). Consequently, it is likely that the high-U zirconolites in 67955 were extensively metamict at the time they were incorporated into ejecta at 3.9 Ga (Norman et al., 2010), making them prone to Pb loss and resetting of the U–Pb system under mild heating, whereas the less metamict low-U zirconolites were capable of preserving the crystallization age of the older impact melt at 4.22 ± 0.01 Ga. In this scenario, apatite in 67955 experienced variable resetting of the U–Pb system, producing a range of cooling ages that are intermediate between those recorded by the low-U and high-U zirconolites (Figs. 7, 8).

The three zirconolite analyses with $^{207}Pb/^{206}Pb$ ages $\geqslant$4.3 Ga are anomalous with respect to this interpretation. Such ages might relate to magmatic activity in the lunar crust (Borg et al., 2011; Grange et al., 2011), but inheritance of relict zirconolite directly from pre-impact target rocks seems unlikely for reasons discussed previously. Xenocrystic zirconolite has not been reported in terrestrial magmatic rocks (Rasmussen and Fletcher, 2004; Rasmussen et al., 2009; Wu et al., 2010) in part because zirconolite reacts rapidly with a silicate melt at temperatures over which 67955 would have crystallized, i.e., $T \geqslant 1200\,^{\circ}C$ (Loiseau et al., 2003b). Alternatively, these older ages may reflect the presence of excess radiogenic lunar lead. Borg et al. (2011) noted the ubiquitous presence in lunar highlands rocks of a component (Pba) with high $^{207}Pb/^{206}Pb$ that is apparently related to evolution of a KREEP reservoir and is a potential contaminant in all lunar samples. Terrestrial contamination can be discounted by the low $^{204}Pb/^{206}Pb$ of these analyses. Although additional studies are needed, we tentatively ascribe these older $^{207}Pb/^{206}Pb$ ages to the presence of anomalous lunar Pb and discount these data in the interpretation presented here.

4.3. Implications for Late Heavy Bombardment and Terminal Cataclysm

The crystallization age of the 67955 noritic anorthosite extends the lunar basin-forming epoch back to at least 4.2 Ga. Although the concept of a short-lived terminal cataclysm is not universally accepted (Chapman et al., 2007), for the first time we now have direct, sample-based geochronological evidence for a basin-scale impact melting event on the Moon prior to 3.9 Ga. This provides a more definitive framework for the interpretation of other evidence for pre-cataclysm impacts on the Moon. Multiple impact events with ages ranging from 3.9 to 4.3 Ga have been inferred from shocked zircons found in a variety of Apollo breccias, lunar meteorites, and regolith samples (Gnos et al., 2004; Pidgeon et al., 2007; Grange et al., 2011; Liu et al., 2012; Zhang et al., 2012). Those ages reflect thermo-mechanical events of sufficient magnitude to reset the U–Pb system in recrystallized or plastically deformed igneous zircon although the P-T-t conditions, and therefore the magnitude of the impact events, that generated those effects are poorly constrained (Grange et al., 2011; Timms et al., 2012). Some lunar metamorphic breccias and fragment-laden melt-breccia clasts yield apparent $^{40}Ar–^{39}Ar$ plateau ages of 4.1–4.3 Ga (Stöffler et al., 1985; Hudgins et al., 2008; Norman et al., 2010; Fernandes et al., 2013), but the question of partial equilibration of inherited clasts in these breccias complicates a straightforward interpretation of those data (Norman et al., 2010). Recently, an impact event at 4.21 ± 0.13 Ga was proposed for lunar melt breccia 67935 based on $^{187}Re–^{187}Os$ isochron data (Fischer-Gödde and Becker, 2012), but the Re–Os isochron approach does not appear generally applicable to dating lunar impact melt rocks (Fischer-Gödde and Becker, 2012) and the geochronological significance of that result has not been independently verified. Fernandes et al. (2013) reported $^{40}Ar–^{39}Ar$ plateau ages of 4.21 ± 0.05 Ga and 4.29 ± 0.04 Ga for two melt breccia fragments extracted from regolith collected at the rim of North Ray crater. Based on the petrography of these samples (Fernandes et al., 2013), they appear to represent relatively small impact events compared to 67955.

The strong version of the late cataclysm hypothesis in which all of the lunar basins formed between 3.8 and 4.0 Ga (Ryder, 2002; Gomes et al., 2005; Abramov and Mojzsis, 2009) appears untenable. Either the geological evidence for older basins has been erased or the oldest lunar basins are $\geqslant$4.2 Ga. It appears that the Moon, and therefore Mars and Earth, experienced an extended phase of post-accretionary heavy bombardment rather than a single short, sharp spike of basin-forming impacts at 3.9 ± 0.1 Ga. In this scenario, the heavy bombardment of the lunar crust began no later than ~4.3 Ga and continued, perhaps episodically, for ~500 million yr, with the terminal cataclysm appearing as the final pulse of an extended period of heavy bombardment. Earlier perceptions of a unique spike of late basin-forming impacts were likely biased by an Imbrium overprint at most if not all of the Apollo sites (Haskin et al., 1998; Norman et al., 2010). A speculative interpretation might be that the late bombardment was episodic with peaks and troughs in the arrival of impactors as envisioned by Tera et al. (1974) in their “Cataclysmic View 2”, and that an earlier episode occurred at or around 4.2–4.3 Ga as reflected in the ages of 67955 and the lunar zircons and granulitic breccias, with a terminal cataclysm at ~3.9 Ga.

Possible implications of an extended episode of heavy bombardment for Solar System dynamics, the environmental conditions on Mars and the early Earth, and planetary surface chronologies based on basin populations may need further consideration. A prolonged period of early bombardment implies relatively benign environmental conditions on the early terrestrial planets, supporting previous conclusions that impact frustration of life was unlikely (Ryder, 2002; Zahnle et al., 2007; Abramov and Mojzsis, 2009), although it is possible that large impacts exerted a significant influence on early biological evolution by imposing major but relatively short-lived excursions on early environmental systems. Analogously, large impacts probably were not the primary agent responsible for destruction of the Hadean crust (cf. Kamber, 2007), and the similar ages proposed for the terminal cataclysm and observed for the oldest extant sialic crust on Earth seem more likely to be coincidental rather than having a genetic significance, as speculated on occasionally (Glikson, 2001). A less intense episode of 3.9 Ga bombardment may also provide at least a partial explanation for the scarcity of impact signatures in the Archean rock record of Earth (Ryder et al., 2000), and additional motivation to search for impact-related features in Hadean samples such as the pre-3.8 Ga zircons found mostly in Western Australia. Abbott et al. (2012) reported higher Ti-temperatures in 3.85–3.95 Ga zircons compared to a set of 3.95–4.10 Ga zircons from the Jack Hills, WA, and suggested that this may represent the only trace of the late heavy bombardment found so far on Earth. In contrast, Bell and Harrison (2013) emphasized a unique population of low-T meta-

morphic zircons with ages of 3.84–3.91 Ga. Both studies ascribed these effects to a possible signature of the late heavy bombardment. Although the time-integrated mass flux for the Hadean remains highly uncertain, broadening the curve also implies that the late veneer of highly siderophile elements in the Earth's mantle was likely emplaced much earlier than 3.9 Ga.

The early dynamical evolution of the solar system may have sampled discrete reservoirs of impactors, which could be recorded in geochemical signatures of lunar melt rocks with a range of ages, and in crater populations on the Moon. Marchi et al. (2012) inferred an increase in the velocities of the impacting bodies associated with Nectarian and Imbrian age lunar basins, possibly reflecting different mechanisms for delivery of early vs. late impactors. Morbidelli et al. (2012) associated this change with a residual population of post-accretionary residual planetesimals and a juvenile population generated by the break-up of E-belt asteroids, respectively. Although Morbidelli et al. (2012) assigned an age of 4.1 Ga to this shift, the timing of any inflection in the model curves is poorly constrained as we still do not have an absolute age that can be assigned with confidence to any of the older lunar basins, including Nectaris. While it seems clear that basin-forming impacts did occur on the Moon (and therefore on Earth and Mars as well) at least as early as 4.2 Ga, our understanding of the mechanisms and consequences of this bombardment remains limited.

5. Conclusions

The U–Pb isotopic compositions of zirconolite and apatite in lunar melt rock 67955 establish a basin-scale impact melting event on the Moon at 4.2 Ga followed by entrainment of the melt rock in lower grade ejecta approximately 300 million yr later. Petrologic and textural characteristics of these accessory phases are more consistent with in situ crystallization from late-stage residual melts rather than inheritance of relict phases from the pre-impact protolith. Their preservation as clasts is also unlikely due to their short survival times relative to the crystallization interval of the coarse-grained, clast-poor impact melt in which they are found. The ages of lunar zircons and metamorphosed breccias also suggest that multiple large impacts occurred on the Moon at around that time, but the sizes of those events is difficult to establish. Perceptions of a unique cataclysmic spike of basin-forming impacts at 3.9 Ga were likely biased by an Imbrium overprint at the Apollo sites, and the terminal cataclysm now appears be the final phase of an extended period of heavy bombardment that began no later than 4.2 Ga and possibly earlier. The strong version of the cataclysm hypothesis in which all lunar basins formed between 3.8 and 4.0 Ga appears to be untenable. A prolonged period of early bombardment implies relatively benign environmental conditions on the early terrestrial planets. Impact frustration of life appears unlikely although large impacts may have exerted a significant influence on early biological evolution by imposing major but short-lived excursions on early environmental systems. The implications of a prolonged period of basin formation for planetary dynamics requires further exploration to evaluate mechanisms for delivery of large impactors to the inner Solar System. The early dynamical evolution of the solar system may have sampled discrete reservoirs of impactors, which could be recorded in geochemical signatures of lunar melt breccias and crater populations on the Moon. This scenario represents a new paradigm for interpreting the early bombardment history of the terrestrial planets and its effects on evolving geological and biological systems.

Acknowledgements

Visiting Scientist support provided by the LPI to MN is gratefully acknowledged. We thank Axel Wittmann, Oleg Abramov, and an anonymous reviewer for comments that improved the manuscript, and Mark Harrison for efficient editorial handling. Financial support was provided by Curtin University. Discussions with W.F. Bottke, W.K. Hartmann, D. Kring, and R. Arculus clarified some concepts and observations presented here.

Appendix A. Supplementary material

Supplementary material related to this article can be found online at http://dx.doi.org/10.1016/j.epsl.2013.11.040.

References

Abbott, S.S., Harrison, T.M., Schmitt, A.K., Mojzsis, S.J., 2012. A search for thermal excursions from ancient extraterrestrial impacts using hadean zircon Ti–U–Th–Pb depth profiles. Proc. Natl. Acad. Sci. USA 109, 13486–13492.
Abramov, O., Mojzsis, S.J., 2009. Microbial habitability of the Hadean Earth during the late heavy bombardment. Nature 459, 419–422.
Abramov, O., Wong, S.M., Kring, D.A., 2012. Differential scaling for oblique impacts on terrestrial planets. Icarus 218, 906–916.
Anand, M., Taylor, L.A., Neal, C.R., Snyder, G.A., Patchen, A., Sano, Y., Terada, K., 2003. Petrogenesis of lunar meteorite EET 96008. Geochim. Cosmochim. Acta 67, 3499–3518.
Anders, E., 1978. Procrustean science: indigenous siderophiles in the lunar highlands, according to Delano and Ringwood. In: Proc. Lunar Planet. Sci. Conf. 9th, pp. 161–184.
Anders, E., Grevesse, N., 1989. Abundances of the elements: meteoritic and solar. Geochim. Cosmochim. Acta 53, 197–214.
Anderson, C.A., Hinthorne, J.R., 1972. U, Th, Pb and REE abundances and $^{207}Pb/^{206}Pb$ ages of individual minerals in returned lunar material by ion microprobe mass analysis. Earth Planet. Sci. Lett. 14, 195–200.
Anderson, C.A., Hinthorne, J.R., 1973. $^{207}Pb/^{206}Pb$ ages of individual mineral phases in Luna 20 material by ion microprobe mass analysis. Geochim. Cosmochim. Acta 37, 745–754.
Ashwal, L.D., 1975. Petrologic evidence for a plutonic igneous origin of anorthositic clasts in 67955 and 77017. In: Proc. Lunar Sci. Conf. 6, pp. 221–230.
Beard, B.L., Ludois, J.M., Lapen, T.J., Johnson, C.M., 2013. Pre-4.0 billion year weathering on Mars constrained by Rb–Sr geochronology on meteorite ALH84001. Earth Planet. Sci. Lett. 361, 173–182.
Bell, E.A., Harrison, T.M., 2013. Post-Hadean transitions in Jack Hills zircon provenance: a signal of the Late Heavy Bombardment?. Earth Planet. Sci. Lett. 364, 1–11.
Bogard, D.D., 1995. Impact ages of meteorites: A synthesis. Meteoritics 30, 244–268.
Bogard, D.D., 2011. K–Ar ages of meteorites: clues to parent body thermal histories. Chem. Erde 71, 207–226.
Borg, L.E., Connelly, J.N., Boyet, M., Carlson, R.W., 2011. Chronological evidence that the Moon is either young or did not have a magma ocean. Nature 477, 70–73.
Cashman, K.V., 1993. Relationship between plagioclase crystallization and cooling rate in basaltic melts. Contrib. Mineral. Petrol. 113, 126–142.
Chapman, C.R., Cohen, B.A., Grinspoon, D.H., 2007. What are the real constraints on the existence and magnitude of the late heavy bombardment?. Icarus 189, 233–245.
Chyba, C.F., Sagan, C., 1992. Endogenous production, exogenous delivery and impact-shock synthesis of organic molecules: An inventory for the origins of life. Nature 355, 125–131.
Cintala, M.J., Grieve, R.A.F., 1998. Scaling impact melting and crater dimensions: implications for the lunar cratering record. Meteorit. Planet. Sci. 33, 889–912.
Cushing, J.A., Taylor, G.J., Norman, M.D., Keil, K., 1999. The granulitic impactite suite: Impact melts and metamorphic breccias of the early lunar crust. Meteorit. Planet. Sci. 34, 185–195.
Dalrymple, G.B., Ryder, G., 1996. Argon-40/argon-39 age spectra of Apollo 17 highlands breccia samples by laser step heating and the age of the Serenitatis basin. J. Geophys. Res. 101, 26069–26084.
Day, J.M.D., Walker, R.J., James, O.B., Puchtel, I.S., 2010. Osmium isotope and highly siderophile element systematics of the lunar crust. Earth Planet. Sci. Lett. 289, 595–605.
Delano, J.W., 1977. Experimental melting relations of 63545, 76015, and 76055. In: Proc. Lunar Sci. Conf. 8th, pp. 2097–2123.
Delano, J.W., Ringwood, A.E., 1978. Siderophile elements in the lunar highlands: nature of the indigenous component and implications for the origin of the Moon. In: Proc. Lunar Planet. Sci. Conf. 9th, pp. 11–159.
Donaldson, C.H., 1976. An experimental investigation of olivine morphology. Contrib. Mineral. Petrol. 57, 187–213.
Dymek, R.F., Albee, A.L., Chodos, A.A., 1975. Comparative petrology of lunar cumulate rocks of possible primary origin: dunite 72415, troctolite 76535, norite 78235, and anorthosite 62237. In: Proc. Lunar Sci. Conf. 6th, pp. 301–341.
Farmer, J.D., 2000. Hydrothermal systems: Doorways to early biosphere evolution. GSA Today 10, 2–9.

Faure, F., Trolliard, G., Nicollet, C., Montel, J.-M., 2003. A developmental model of olivine morphology as a function of the cooling rate and the degree of undercooling. Contrib. Mineral. Petrol. 145, 251–263.

Fernandes, V.A., Fritz, J., Weiss, B.P., Garrick-Bethell, I., Shuster, D.L., 2013. The bombardment history of the Moon as recorded by ^{40}Ar–^{39}Ar chronology. Meteorit. Planet. Sci., 1–29. http://dx.doi.org/10.1111/maps.12054.

Fischer-Gödde, M., Becker, H., 2012. Osmium isotope and highly siderophile element constraints on ages and nature of meteoritic components in ancient lunar impact rocks. Geochim. Cosmochim. Acta 77, 135–156.

French, B.M., 1998. Traces of a Catastrophe. LPI Contrib. 954. 120 pp. http://www.lpi.usra.edu/publications/books/CB-954/CB-954.intro.html.

Gilbert, S., Danyushevsky, L., Robinson, P., Wohlgemuth-Ueberwasser, C., Pearson, N., Savard, D., Norman, M., Hanley, J., 2012. A comparative study of five reference materials and the Lombard meteorite for the determination of the platinum-group elements and gold by LA-ICP-MS. Geostand. Geoanal. Res. 37 (1), 51–64. http://dx.doi.org/10.1111/j.1751-908X.2012.00170.x.

Glikson, A.Y., 2001. The astronomical connection of terrestrial evolution: crustal effects of post-3.8 Ga mega-impact clusters and evidence for major 3.2 ± 0.1 Ga bombardment of the Earth–Moon system. J. Geodyn. 32, 205–229.

Gnos, E., Hofmann, B.A., Al-Kathiri, A., Lorenzetti, S., Eugster, O., Whitehouse, M.J., Villa, I.M., Jull, A.J.T., Eikenberg, J., Spettel, B., Kranhenbuhl, U., Franchi, I.A., Greenwood, R.C., 2004. Pinpointing the source of a lunar meteorite: implications for the evolution of the Moon. Science 305, 657–659.

Gomes, R., Levison, H.F., Tsiganis, K., Morbidelli, A., 2005. Origin of the cataclysmic Late Heavy Bombardment period of the terrestrial planets. Nature 435, 466–469.

Grange, M.L., Nemchin, A.A., Timms, N., Pidgeon, R.T., Meyer, C., 2011. Complex magmatic and impact history prior to 4.1 Ga recorded in zircon from Apollo 17 South Massif aphanitic breccia 73235. Geochim. Cosmochim. Acta 75, 2213–2232.

Haines, E.L., Albee, A.L., Chodos, A.A., Wasserburg, G.J., 1971. Uranium-bearing minerals in lunar rock 12013. Earth Planet. Sci. Lett. 12, 145–154.

Harrison, T.M., Watson, E.B., 1984. The behavior of apatite during crustal anatexis: equilibrium and kinetic considerations. Geochim. Cosmochim. Acta 48, 1467–1477.

Hartmann, W.K., 2003. Megaregolith evolution and cratering cataclysm models – Lunar cataclysm as a misconception (28 years later). Meteorit. Planet. Sci. 38, 579–593.

Haskin, L.A., Korotev, R.L., Rockow, K., Jolliff, B.L., 1998. The case for an Imbrium origin of the Apollo thorium-rich impact-melt breccias. Meteorit. Planet. Sci. 33, 959–975.

Hess, P.C., Rutherford, M.J., Campbell, H.W., 1978. Ilmenite crystallization in nonmare basalt: genesis of KREEP and high-Ti mare basalt. In: Proc. Lunar Planet. Sci. Conf. 9th, pp. 705–724.

Hinthorne, J.R., Andersen, C.A., Conrad, R.L., Lovering, J.F., 1979. Single-grain ^{207}Pb/^{206}Pb and U/Pb age determinations with a 10 μm spatial resolution using the ion microprobe mass analyzer (IMMA). Chem. Geol. 25, 271–303.

Hodges, C.A., Muehlberger, W.R., Ulrich, G.E., 1973. Geologic setting of Apollo 16. In: Proc. Lunar Sci. Conf. 4th, pp. 1–25.

Hollister, L.S., 1973. Sample 67955: a description and a problem. In: Proc. Lunar Sci. Conf. 4, pp. 633–641.

Hudgins, J.A., Spray, J.G., Kelley, S.P., Korotev, R.L., Sherlock, S.C., 2008. A laserprobe ^{40}Ar/^{39}Ar and INAA investigation of four Apollo granulitic breccias. Geochim. Cosmochim. Acta 72, 5781–5798.

James, O.B., 1980. Rocks of the early lunar crust. In: Proc. Lunar Planet. Sci. Conf. 11th, pp. 365–393.

James, O.B., Flohr, M.K., 1983. Subdivision of the Mg-suite noritic rocks into Mg-gabbronorites and Mg-norites. In: Proc. Lunar Planet. Sci. Conf. 13th. J. Geophys. Res. 88 Suppl., A603–A614.

Jourdan, F., 2012. The 40Ar/39Ar dating technique applied to planetary sciences and terrestrial impacts. Aust. J. Earth Sci. 59, 199–224.

Joy, K.H., Burgess, R., Hinton, R., Fernandes, V.A., Crawford, I.A., Kearsley, A.T., Irving, A.J., 2011. Petrogenesis and chronology of lunar meteorite Northwest Africa 4472: a KREEPy regolith breccia from the Moon. Geochim. Cosmochim. Acta 75, 2420–2452.

Kamber, B.S., 2007. The enigma of the terrestrial protocrust: evidence for its former existence and the importance of its complete disappearance. In: van Kranendonk, M.J., Smithes, H.R.H., Bennett, V.C. (Eds.), Earth's Oldest Rocks. In: Developments in Precambrian Geology, vol. 15. Elsevier, pp. 75–90.

Lesher, C.E., Cashman, K.V., Mayfield, J.D., 1999. Kinetic controls on crystallization of Tertiary North Atlantic basalt and implications for the emplacement and cooling history of lava at Site 989, Southeast Greenland rifted margin. In: Proc. International Ocean Drilling Program 163 Scientific Results. Available from http://www-odp.tamu.edu/publications/163_SR/163TOC.HTM.

Lisse, C.M., Wyatt, M.C., Chen, C.H., Morlok, A., Watson, D.M., Manoj, P., Sheehan, P., Currie, T.M., Thebault, P., Sitko, M.L., 2012. Spitzer evidence for a late heavy bombardment and the formation of ureleites in η Corvi at ~1 Gyr. Ap. J. 747, 93–118.

Liu, D., Jolliff, B.L., Zeigler, R.A., Korotev, R.L., Wan, Y., Xie, H., Zhang, Y., Dong, C., Wang, W., 2012. Comparative zircon U–Pb geochronology of impact melt breccias from Apollo 12 and lunar meteorite SaU 169, and implications for the age of the Imbrium impact. Earth Planet. Sci. Lett. 319–320, 277–286.

Loiseau, P., Caurant, D., Majerus, O., Baffier, N., Fillet, C., 2003a. Crystallization study of (TiO_2–ZrO_2)-rich SiO_2–Al_2O_3–CaO glasses. Part 1. Preparation and characterization of zirconolite-based glass-ceramics. J. Mater. Sci. 38, 843–852.

Loiseau, P., Caurant, D., Majerus, O., Baffier, N., Fillet, C., 2003b. Crystallization study of (TiO_2–ZrO_2)-rich SiO_2–Al_2O_3–CaO glasses. Part II. Surface and internal crystallization processes investigated by differential thermal analysis (DTA). J. Mater. Sci. 38, 853–864.

Lovering, J.F., Wark, D.A., 1971. Uranium-enriched phases in Apollo 11 and Apollo 12 basaltic rocks. Proc. Lunar Sci. Conf. 2, 151–158.

Lumpkin, G.R., Ewing, R.C., Chakoumakos, B.C., Greegor, R.B., Lytle, F.W., Foltyn, E.M., Clinard, F.W., Boatner, L.A., Abraham, M.M., 1986. Alpha-recoil damage in zirconolite ($CaZrTi_2O_7$). J. Mater. Res. 1, 564–576.

Marchi, S., Bottke, W.F., Kring, D.A., Morbidelli, A., 2012. The onset of the lunar cataclysm as recorded in its ancient crater populations. Earth Planet. Sci. Lett. 325–326, 27–38.

Marty, B., Meibom, A., 2007. Noble gas signature of the Late Heavy Bombardment in the Earth's atmosphere. Earth 2, 43–49.

Meyer, C., 2010. The lunar sample compendium. Available from http://curator.jsc.nasa.gov/lunar/compendium.cfm.

Morbidelli, A., Chambers, J., Lunine, J.I., Petit, J.M., Robert, F., Valsecchi, G.B., Cyr, K.E., 2000. Source regions and timescales for the delivery of water to the Earth. Meteorit. Planet. Sci. 35, 1309–1320.

Morbidelli, A., Marchi, S., Bottke, W.F., Kring, D.A., 2012. A sawtooth-like timeline for the first billion years of lunar bombardment. Earth Planet. Sci. Lett. 355–356, 144–151.

Naldrett, A.J., Bray, J.G., Gasparrini, E.L., Podolsky, T., Rucklidge, J.C., 1970. Cryptic variation and the petrology of the Sudbury Nickel Irruptive. Econ. Geol. 65, 122–155.

Nemchin, A.A., Pidgeon, R.T., Healey, D., Grange, M.L., Whitehouse, M.J., Vaughan, J., 2009. Comparative behavior of apatite–zircon U–Pb systems in Apollo 14 breccias: implications for the thermal history of the Fra Mauro Formation. Meteorit. Planet. Sci. 44, 1717–1734.

Nord, G.L., Christie, J.M., Heuer, A.H., Lally, J.S., 1975. North Ray Crater breccias: An electron petrographic study. In: Proc. Lunar Sci. Conf. 6th, pp. 779–797.

Norman, M.D., Ryder, G., 1979. A summary of the petrology and geochemistry of pristine highlands rocks. In: Proc. Lunar Planet. Sci. Conf. 10th, pp. 531–559.

Norman, M.D., Duncan, R.A., Huard, J.J., 2006. Identifying impact events within the lunar cataclysm from ^{40}Ar–^{39}Ar ages and compositions of Apollo 16 impact melt rocks. Geochim. Cosmochim. Acta 70, 6032–6049.

Norman, M.D., Shih, C.-Y., Nyquist, L.E., Bogard, D.D., Taylor, L.A., 2007. Early impacts on the Moon: Crystallization ages of Apollo 16 melt breccias (abs. #1991). In: Lunar Planet. Sci. XXXVIII. Lunar Planetary Institute, Houston.

Norman, M.D., Duncan, R.A., Huard, J.J., 2010. Imbrium provenance for the Apollo 16 Descartes terrain: argon ages and geochemistry of lunar breccias 67016 and 67455. Geochim. Cosmochim. Acta 74, 763–783.

O'Connell-Cooper, C.D., Spray, J.G., 2011. Geochemistry of the impact-generated melt sheet at Manicouagan: evidence for fractional crystallization. J. Geophys. Res. 116, B06204. http://dx.doi.org/10.1029/2010JB008084.

Palme, H., 1980. The meteoritic contamination of terrestrial and lunar impact melts and the problem of indigenous siderophiles in the lunar highland. In: Proc. Lunar Planet. Sci. Conf. 11th, pp. 481–506.

Pan, Y., 1997. Zircon- and monazite-forming metamorphic reactions at Manitouwadge, Ontario. Can. Mineral. 35, 105–118.

Peckett, A., Phillips, R., Brown, G.M., 1972. New zirconium-rich mineral from Apollo 14 and 15 lunar rocks. Nature 236, 215–217.

Pidgeon, R.T., Nemchin, A.A., van Bronswijk, W., Geisler, T., Meyer, C., Compston, W., Williams, I.S., 2007. Complex history of a zircon aggregate from lunar breccia 73235. Geochim. Cosmochim. Acta 71, 1370–1381.

Rasmussen, B., Fletcher, I.R., 2004. Zirconolite: a new U–Pb chronometer for mafic igneous rocks. Geology 32, 785–788.

Rasmussen, B., Fletcher, I.R., Muhling, J.R., 2008. Pb/Pb geochronology, petrography and chemistry of Zr-rich accessory minerals (zirconolite, tranquillityite and baddeleyite) in mare basalt 10047. Geochim. Cosmochim. Acta 72, 5799–5818.

Rasmussen, B., Mueller, A.G., Fletcher, I.R., 2009. Zirconolite and xenotime U–Pb age constraints on the emplacement of the Golden Mile dolerite sill and gold mineralization at the Mt. Charlotte mine, eastern Goldfields Province, Yilgarn craton, Western Australia. Contrib. Mineral. Petrol. 157, 559–572.

Reimold, W.U., Gibson, R.L., 2006. The melt rocks of the Vredefort impact structure—Vredefort granophyre and pseudotachylitic breccias: implications for impact cratering and the evolution of the Witwatersrand Basin. Chem. Erde 66, 1–35. http://dx.doi.org/10.1016/j.chemer.2005.07.003.

Ryder, G., 1979. The chemical components of highlands breccias. In: Proc. Lunar Planet. Sci. Conf. 10th, pp. 561–581.

Ryder, G., 2002. Mass flux in the ancient Earth–Moon system and benign implications for the origin of life on Earth. J. Geophys. Res. 107. http://dx.doi.org/10.1029/2001JE001583.

Ryder, G., Norman, M.D., Score, R.A., 1980. The distinction of pristine from meteorite-contaminated highlands rocks using metal compositions. In: Proc. Lunar Planet. Sci. Conf. 11th, pp. 471–479.

Ryder, G., Koeberl, C., Mojzsis, S.J., 2000. Heavy bombardment on the Earth at ~3.85 Ga: the search for petrographic and geochemical evidence. In: Canup,

R.M., Righter, K. (Eds.), Origin of the Earth and Moon. U. Arizona Press, Tucson, pp. 475–492.
Simonds, C.H., 1975. Thermal regimes in impact melts and the petrology of the Apollo 17 Station 6 boulder. In: Proc. Lunar Sci. Conf. 6th, pp. 641–672.
Simonds, C.H., Warner, J.L., Phinney, W.C., 1973. Petrology of Apollo 16 poikilitic rocks. In: Proc. Lunar Sci. Conf. 4th, pp. 613–632.
Simonds, C.H., Warner, J.L., Phinney, W.C., McGee, P.E., 1976. Thermal model for impact breccia lithification: Manicouagan and the Moon. In: Proc. Lunar Sci. Conf. 7th, pp. 2509–2528.
Stern, R.A., Bodorkos, S., Kamo, S.L., Hickman, A.H., Corfu, F., 2009. Measurement of SIMS instrumental mass fractionation of Pb isotopes during zircon dating. Geostand. Geoanal. Res. 33, 145–168.
Stöffler, D., Bischoff, A., Borchardt, R., Burghele, A., Deutsch, A., Jessberger, E.K., Ostertag, R., Palme, H., Spettel, B., Reimold, W.U., Wacker, K., Wänke, H., 1985. Composition and evolution of the lunar crust in the Descartes highlands. In: Proc. Lunar Planet. Sci. Conf 15th. J. Geophys. Res. 90, C449–C506.
Stöffler, D., Ryder, G., Ivanov, B.A., Artemieva, N.A., Contala, M.J., Grieve, R.A.F., 2006. Cratering history and lunar chronology. In: Jolliff, B.L., Wieczorek, M.A., Shearer, C.K., Neal, C.R. (Eds.), New Views of the Moon. In: Reviews in Mineralogy and Geochemistry, vol. 60, pp. 519–596. Chapter 5.
Strom, R.G., Malhotra, R., Ito, T., Yoshida, F., Kring, D.A., 2005. The origin of planetary impactors in the inner solar system. Science 309, 1847–1850.
Tera, F., Papanastassiou, D.A., Wasserburg, G.J., 1974. Isotopic evidence for a terminal lunar cataclysm. Earth Planet. Sci. Lett. 22, 1–21.
Terada, K., Sasaki, T., Anand, M., Joy, K.H., Sano, Y., 2007. Uranium-lead systematic of phosphates in lunar basaltic regolith breccia, Meteorite Hills 01210. Earth Planet. Sci. Lett. 259, 77–84.
Therriault, A.M., Fowler, A.D., Grieve, R.A.F., 2002. The Sudbury Igneous Complex: a differentiated impact melt sheet. Econ. Geol. 97, 1521–1540.
Timms, N.E., Reddy, S.M., Healy, D., Nemchin, A.A., Grange, M.L., Pidgeon, R.T., Hart, R., 2012. Resolution of impact-related microstructures in lunar zircon: a shock-deformation mechanism map. Meteorit. Planet. Sci. 47, 120–141.
Van Orman, J.A., Grove, T.L., 2000. Origin of lunar high-titanium ultramafic glasses: constraints from phase relations and dissolution kinetics of clinopyroxene-ilmenite cumulates. Meteorit. Planet. Sci. 35, 783–794.
Walker, D., Longhi, J., Hays, J., 1972. Experimental petrology and the origin of Fra Mauro rocks and soils. In: Proc. Lunar Sci. Conf. 3rd, pp. 797–817.
Walker, D., Longhi, J., Grove, T.L., Stolper, E., Hays, J.F., 1973. Experimental petrology and origin of rocks from the Descartes highlands. In: Proc. Lunar Sci. Conf. 4th, pp. 1013–1032.
Wagner, T.P., Grove, T.L., 1997. Experimental constraints on the origin of lunar high-Ti ultramafic glasses. Geochim. Cosmochim. Acta 61, 1315–1327.
Wänke, H., Dreibus, G., Palme, H., 1978. Primary matter in the lunar highlands: the case of the siderophile elements. In: Proc. Lunar Planet. Sci. Conf. 9th, pp. 83–110.
Warner, J.L., Phinney, W.C., Simonds, C.H., 1976. Apollo 17, Station 6 boulder sample 76255 – Absolute petrology of breccia matrix and igneous clasts. In: Proc. Lunar Sci. Conf. 7th, pp. 2233–2250.
Warner, J.L., Phinney, W.C., Bickel, C.E., Simonds, C.H., 1977. Feldspathic granulitic impactites and pre-final bombardment lunar evolution. In: Proc. Lunar Sci. Conf. 8th, pp. 2051–2066.
Warren, P.H., 1993. A concise compilation of petrologic information on possibly pristine nonmare Moon rocks. Am. Mineral. 78, 360–376.
Warren, P.H., 2011. Ejecta-megaregolith accumulation on planetesimals and large asteroids. Meteorit. Planet. Sci. 46, 53–78.
Warren, P.H., Claeys, P., Cedillo-Pardo, E., 1996. Mega-impact melt petrology (Chicxulub, Sudbury, and the Moon): effects of scale and other factors on potential for fractional crystallization and development of cumulates. In: Ryder, G., Fastovsky, D., Gartner, S. (Eds.), The Cretaceous-Tertiary Event and Other Catastrophes in Earth History. In: Geological Society of America Special Paper, vol. 307. Geological Society of America, Boulder, Colorado, pp. 105–124.
Watson, E.B., 1979. Apatite saturation in basic to intermediate magmas. Geophys. Res. Lett. 6, 937–940.
Wielicki, M.M., Harrison, T.M., Schmitt, A.K., 2012. Geochemical signatures and magmatic stability of terrestrial impact produced zircon. Earth Planet. Sci. Lett. 321–322, 20–31.
Wu, F.-Y., Yang, Y.H., Mitchell, R.H., Bellatreccia, F., Li, Q.-L., Zhao, Z.-F., 2010. In situ U–Pb and Nd–Hf–(Sr) isotopic investigations of zirconolite and calzirtite. Chem. Geol. 277, 178–195.
Zahnle, K., Arndt, N., Cockell, C., Halliday, A., Nesbet, E., Selsis, F., Sleep, N.H., 2007. Emergence of a habitable planet. Space Sci. Rev. 129, 35–78.
Zhang, A.-C., Hsu, W.-B., Li, Q.-L., Liu, Y., Jiang, Y., Tang, G.-Q., 2010. SIMS Pb/Pb dating of Zr-rich minerals in lunar meteorites Miller Range 05035 and LaPaz Icefield 02224: Implications for the petrogenesis of mare basalt. Sci. China Earth Sci. 53, 327–334.
Zhang, A.-C., Taylor, L.A., Wang, R.-C., Li, Q.-L., Li, X.-H., Patchen, A.D., Liu, Y., 2012. Thermal history of Apollo 12 granite and KREEP-rich rock: Clues from Pb/Pb ages of zircon in lunar breccia 12013. Geochim. Cosmochim. Acta 95, 1–14.